Understanding microbial sourcing in Greenland subglacial runoff

Guillaume Lamarche-Gagnon[1,2*], Marek Stibal[3], Alexandre M. Anesio[4], Jemma L. Wadham[1,2], Jon R. Hawkings[1,5], Lukáš Falteisek[3], Kristýna Vrbická[3], Petra Klímová[3], Jakub D. Žárský[3], Tyler J. Kohler[3], Elizabeth A. Bagshaw[2], Jade E. Hatton[3], Alexander D. Beaton[6], Jon Telling[7]

[1]Centre for ice, Cryosphere, Carbon and Climate (iC3), Department of Geosciences, UiT The Arctic University of Norway, 9037 Tromsø, Norway
[2]School of Geographical Sciences, University of Bristol, Bristol BS8 1SS, UK
[3]Department of Ecology, Faculty of Science, Charles University, Prague, 128 44, Czechia
[4]Department of Environmental Science, Aarhus University, Aarhus, 4000 Roskilde, Denmark
[5]Department of Earth and Environment, University of Pennsylvania, Philadelphia, PA, USA
[6]Ocean Technology and Engineering Group, National Oceanography Centre, Southampton, UK
[7]School of Natural and Environmental Sciences, Newcastle University, Newcastle, UK

*Correspondance to: Guillaume Lamarche-Gagnon (guillaume.lamarche-gagnon@uit.no)

Abstract. The microbial ecosystems that lie beneath ice sheets can impact and contribute to global biogeochemical cycles, yet remain poorly understood given the logistical challenges in directly accessing the subglacial environment. Studies instead often rely on indirect sampling of subglacial systems via the collection of meltwaters emerging from ice margins. However, the origin of exported material in these waters will change over a melt season as glacier hydrology responds to changes in surface melt. Here, we reveal trends in microbial sourcing (source environment) and assemblages in a large proglacial river in southwest Greenland by investigating three microbial datasets (16S rRNA) collected during different hydrological periods over three separate summer melt seasons. By combining microbial data with high-resolution hydrological and hydrochemical measurements, we show that changes in microbial assemblages follow changes in hydrological periods, likely influenced by variations in glacial drainage expansion inland with concomitant variations in inputs of surface melt and subglacial sediment exports. We further illustrate how relative changes in microbial assemblages can inform on the state of the glacial hydrological system, and also focus on methane-cycling populations to infer their potential distribution beneath the ice. Overall, our results highlight that timing matters when sampling proglacial rivers and we caution interpretations of exported assemblages without a good understanding of the catchment and system studied; this is especially true for larger systems which undergo more complex hydrological changes over a melt season.

1 Introduction

The beds of glaciers and ice sheets are now recognised as widespread ecosystems conducive to biochemical and biogeochemical reactions with impacts well beyond the ice margins (Wadham et al., 2019; Christner et al., 2014). Subglacial ecosystems promote chemical weathering reactions, leading to the potential release of nutrients (e.g. Si, Fe) and heavy metals (e.g. Hg) to proglacial zones and nearby fjords and oceans (e.g. Graly et al., 2017; Hawkings et al., 2021b; Hawkings et al., 2014), and the generation and build-up of subglacial greenhouse gas reserves (methane) that can leak to the atmosphere (e.g. Burns et al., 2018; Lamarche-Gagnon et al., 2019; Christiansen and Jørgensen, 2018; Pain et al., 2019). Despite this importance, our understanding of subglacial

40   microbial processes and communites remains limited, hindered by the difficulty to directly access the subglacial

41   environment.

42

43   An increasing number of studies have circumvented this logistical challenge by sampling subglacial material in

44   meltwaters exported from the ice margin. In most glacial systems, such as those found in the ablation zone of the

45   Greenland Ice Sheet (GrIS), surface melt reaches the bed of the ice sheet before exiting glaciers at their front; for

46   land-terminating glaciers, glacial runoff ultimately takes the form of proglacial rivers. During the melt season,

47   these rivers can therefore offer indirect access to the subglacial environment, and concomitantly to the microbial

48   habitats it encompasses (e.g. Dieser et al., 2014; Kohler et al., 2020; Cameron et al., 2017; Žárský et al., 2018;

49   Dubnick et al., 2017). However, the origin of exported material changes over an ablation season as increasing

50   surface melt re-organises subglacial drainage pathways following snowline retreats on the glacier surface.

51

52   Glaciers with temperate ice regions in Greenland typically undergo a transition from slow and inefficient

53   subglacial drainage (distributed system) during the early part of the melt season, with meltwater during this period

54   normally sourced from sectors of the ice sheet closer to the margin, to efficient fast-flow subglacial drainage in

55   later months draining a larger catchment area and more remote inland sectors of the bed (channelised system;

56   Röthlisberger, 1972; Weertman, 1972; Davison et al., 2019). The degree of mixing between surface melt and the

57   subglacial environment subsequently varies, influencing the quantity and the origin of subglacial material that is

58   transported to the ice margin. Proglacial rivers are consequently sourced from waters of varying residence time

59   beneath the ice and from different sectors of the bed, depending on the state of the hydrological system, which

60   makes disentangling the origin of exported material challenging, and often speculative. Timing of sampling can

61   therefore influence, and potentially skew, interpretations if no additional information on the state of the glacier's

62   hydrological system is considered. This is especially true for larger glacial systems, which undergo more dramatic,

63   pronounced and complex hydrological change throughout the melt season, draining more expansive areas, and

64   likely exporting older, more isolated bed material to the proglacial zone as meltwater generation increases

65   (Wadham et al., 2010; Kohler et al., 2017).

66

67   Here, we provide a detailed investigation into the microbiome of the proglacial river draining the Leverett Glacier

68   (LG), a very well studied large land-terminating glacier of the southwestern sector of the GrIS. We evaluate

69   changes in microbial assemblages (16S rRNA gene) exported from beneath the catchment as the glacier undergoes

70   changes in hydrological connectivity during the first half of the 2015 melt season (e.g. Lamarche-Gagnon et al.,

71   2019; Hatton et al., 2019; Kohler et al., 2017), and also re-visit data from 2017 during late-melt as well as in early

72   to mid summer 2018 before peak flow (Vrbická et al., 2022; Kohler et al., 2020), in order to capture inter-annual

73   variability and a wider range of hydrological periods over three separate summer melt seasons. We assess observed

74   changes based on combined biogeochemical, hydrological, and microbiological data to qualitatively gauge the

75   degree of mixing and homogenisation between different components of the drainage system (e.g. from waters of

76   different residence time subglacially) occurring during fluvial transport upstream of the sampling site.

77   Futhermore, we evaluate whether changes in exported assemblages might point to the existence of different

78   habitats or geochemical conditions in the subglacial catchment and demonstrate that microbiological data can

79   supplement more traditional geochemical and hydrological data to better understand the glacial hydrological

80   system during certain sampling periods. Given the increased attention surrouding glacial emissions of microbial

81   methane from this sector of the ice-sheet (e.g. Stibal et al., 2012; Lamarche-Gagnon et al., 2019; Christiansen and

82   Jørgensen, 2018; Pain et al., 2019; Dieser et al., 2014), we further apply these interpretations to focus on putative

83   methane-cycling populations to see what additional information can be gained about methane cycling beneath the

84   GrIS.

85   **2 Methods**

86   **2.1 Site description**

87   The hydrology and hydrochemistry of Leverett Glacier (LG) have been extensively documented over the last

88   decade (Clason et al., 2015; Chandler et al., 2013; Bartholomew et al., 2011; Hawkings et al., 2021b; Kohler et

89   al., 2017; Hawkings et al., 2014). LG is a polythermal, land-terminating glacier draining a subglacial catchment

90   of ~600-1200 km^2 in the southwestern margin of the GrIS (Cowton et al., 2012; Palmer et al., 2011; Hawkings et

91   al., 2021b). LG overlies Precambrian orthogneiss and granite, common lithology to much of Greenland (Dawes,

92   2009), and its proglacial river, sampled here, is the main source of the Akuliarusiarsuup Kuua, itself a tributary,

93   alongside the Qinnguata Kuussua, to the Watson River near the settlement of Kangerlussuaq. Over the course of

94   a melt season, the catchment undergoes spatial hydrological expansion with processes characteristic of the western

95   margin of the GrIS (details in the Results section below; Davison et al., 2019; Chandler et al., 2013).

96   **2.2 Hydrological and hydrochemical data**

97   All hydrological sensor and hydrochemical data presented here have been described in detail elsewhere (Hawkings

98   et al., 2021b; Kohler et al., 2017). Briefly, continuous measurements of water discharge and suspended sediment

99   concentrations were achieved via the deployment of hydrological sensors for stage (HOBO Onset or Keller DCX-

100 22-CTD) and turbidity (Partech C connected to Campbell CR1000 logger or Turner Cyclops-7F connected to

101 Campbell CR1000 logger) over the span of the 2015 and 2018 sampling periods. Stage was converted to discharge

102 via calibration against a rating curve constructed from manual rhodamine dye injections; turbidity was converted

103 to suspended sediment concentrations (SSC) via calibration against manual samples filtered on pre-weighed

104 cellulose nitrate filters. In 2015, the discharge record at LG spanned the entirety of the melt season, allowing to

105 better contextualise the microbiological sampling period relative to the rest of the melt season. To allow for similar

106 comparisons for the 2017 samples and the 2018 sampling period, we also include complete discharge records

107 from the Watson River (Van As, 2022), of which the LG river is a main tributary (~25 – 65 % of overall Watson

108 daily discharge for the overlapping measurement period), and consequently discharge between the two sites follow

109 very similar patterns (Fig. 1).

110

111 Hydrochemical data collected in parallel to microbiological samples have also been described elsewhere

112 (Hawkings et al., 2021b; Kohler et al., 2020; Kellerman et al., 2020; Hatton et al., 2019; Lamarche-Gagnon et al.,

113 2019; Kohler et al., 2017). Here, we also include dissolved silica (DSi), major ion (MI) and dissolved methane

114 (CH$_{4(aq)}$) concentrations, as well as dissolved oxygen, pH, and electrical conductivity (EC) data for the early May

115 2015 samples collected via ice borehole and chainsawed holes directly in front of the LG terminus (<10 m) prior

116 to glacial melt onset (Table S1; Lamarche-Gagnon et al., 2019). Borehole water samples for DSi, MI and CH$_{4(aq)}$

117 anlayses were first collected using a peristaltic pump (Portapump-810, Williamson Manufacturing) equipped with
118 pre-autoclaved silicon tubing extensively flushed with sample water (> 2 L) prior to sample collection. $CH_{4(aq)}$
119 samples were directly added to pre-evacuated borosilicate vials and analysed as described in Lamarche-Gagnon
120 et al. (2019); subsamples for DSi and major ions were kept cold and then filtered through 0.45 µm cellulose nitrate
121 membrane filters within 2 to 5 hours of collection and analysed as per Hatton et al. (2019). Dissolved oxygen
122 (DO), pH, and EC were only measured for water collected on 4 May 2015 by deploying hydrological sensors
123 through the borehole at ~3-5 meters beneath the river-ice surface; sensors (Aanderaa 3830 for DO, Campbell 247
124 for EC, and Honeywell Durafet for pH) are described in Beaton et al. (2017).

125 **2.3 Microbiological sampling**

126 Except for three samples collected beneath or on river ice in early May and June 2015, respectively (see below),
127 all samples consisted of LG bulk proglacial runoff collected from the river bank. Due to logistical reasons, water
128 volumes and collection sites alongside the LG proglacial river differed slightly between sampling periods and
129 melt seasons but were broadly within 2 km of the glacier terminus (Fig S1, Table S2). In 2015, the sampling
130 period spanned from 4 May to 26 July 2015, with most samples collected ~500 m from the ice margin, except for
131 the first four sets of samples. The first three sets of samples in early May (4-13 May 2015) consisted of relatively
132 stagnant waters collected through naled river ice accessed via a borehole and a chainsawed hole as described in
133 the above section. The following set of samples (7 June) were also collected near the glacier's margin (<20 m)
134 onto river ice, but this time consisted of flowing waters emerging through the river ice in the form of an upwelling
135 that fed the proglacial river at that time. The remaining of the 2015 samples (n=41) were collected from the river
136 bank < 500 m from the ice margin. In 2017, samples (n=3) were collected during a single day during the late melt
137 season near the ice margin (5 September 2017; Kohler et al., 2020). In 2018, the sampling period spanned from
138 21 June to 13 July, with samples collected ~ 2 km from the ice margin (Vrbická et al., 2022).

139

140 All water samples were filtered onto Sterivex filters (0.22 µm, Millipore, Billerica, MA, United States), collected
141 either using sterile 60 mL plastic syringes (2017 and 2018 and most 2015 samples, n = 45) or a peristaltic pump
142 (as described above; 2015 samples, n = 13). Sterivex filters were preserved in MoBio RNA LifeGuard solution
143 (MoBio Laboratories, USA) immediately after sampling and frozen inside a portable freezer (<-10°C) within 1
144 hour of collection. Most water samples collected in 2018 consisted of a single sterivex filter per sampling event,
145 and all 2017 and most 2015 samples were collected in replicates (Table 1/S2). Details on sampling time, location,
146 methods, filtered water volume (usuallly filtered until clogging), and sample replicates are summarised in Table
147 S2.

148

149 Importantly, we maintain that these minor differences in sampling locations and sample processing have little to
150 no measurable impact on microbial composition given that LG subglacial runoff by far consitutes the majority of
151 the discharge of the proglacial river sampled. No major tributary to the LG proglacial river exists within the first
152 2 km of the river, and the area of the catchment that is non-glaciated (~ 11 km2; Vrbická et al., 2022) is orders of
153 magnitude smaller than the overall LG glacial catchment sourcing the proglacial river (~ 840 km2; Hawkings et
154 al., 2021b). Moreover, the relatively fast flowing waters (~1 m s^{-1}) and substantial discharge (often >100s m^3 s^{-1};
155 Fig. 1) would not allow for any meaningful ecological processes to occur within the first 2 km of river sampled.

2.4 DNA extraction and sequencing

DNA from all samples was extracted using the PowerWater Sterivex DNA isolation kit (MO BIO) following the manufactuer's protocol; the 2015 DNA extracts were further purified using the Genomic DNA Clean & Concentrator (Zymo Research, Irvine, CA, USA) as in Žárský et al. (2018) (Lamarche-Gagnon et al., 2019; Vrbická et al., 2022; Kohler et al., 2020). In 2015, extracted DNA samples were then pooled into triplicates for dates when more than 3 Sterivex water samples were collected. For 3 sets of samples, DNA extracts from different (but consecutive) time points were pooled into triplicates (20-23 June, 13-17 July, 21-26 July 2015); Tables 1 and S2 summarises grouping and pooling of the different DNA samples prior to sequencing.

Amplification and sequencing for all samples targeted the V4 region (515-806) of the 16S rRNA gene and performed on a an Illumina MiSeq platform (2 X 250 bp). 2015 and 2017 DNA samples were sequenced at the Mr. DNA laboratory (Shallowater, TX, USA) and amplified using the Caporaso et al. (2011) 515F (GTG**C**CAGCMGCCGCGGTAA) and 806R (GGACTAC**H**VGGGTWTCTAAT) primer pair. 2018 samples were sequenced at SEQme s.r.o. (Dobříš, Czechia) but using the slightly modified Parada et al. (2016) 515F-Y (GTG**Y**CAGCMGCCGCGGTAA) and Apprill et al. (2015) 806R (GGACTAC**N**VGGGTWTCTAAT) primer pair. We acknowledge that the comparison of separate datasets generated using different primer pairs can introduce a degree of primer bias. However, we consider that the difference in primer pairs here should only have a minor impact on the overall sequencing results given the Parada and Apprill primer pair was designed to improve the detection of SAR11 marine taxa and freshwater bacterioplanktons, as well as Crenarchaeota/Thaumarchaeota, clades not expected to make up a large component, if at all, of the subglacial microbial communities investigated here (e.g. Vrbická et al., 2022; Cameron et al., 2017; Henson et al., 2018).

2.5 Bioinformatics analyses

A pre-selection of samples was first made based on a prior screening of the 2015 and 2018 datasets to exclude samples with relatively low numbers of reads per sample. This resulted in an initial sample set (including replicates) of 31 samples for 2015, 3 samples for 2017, and 13 samples for 2018 (compared to 29 LG samples included in Vrbická et al. (2022)) before bioinformactics processing (final processed sample numbers below).

Raw sequences were then uploaded on a remote server and analysed using the mothur platform for preprossessing (Linux v.1.42.3; Schloss et al., 2009). Paired reads were first converted into contigs for each dataset separately, before being merged into a single dataset (*see supplementary information*). Analyses then mostly followed the mothur MiSeq standard operating procedure performed in "batch mode" (https://mothur.org/wiki/miseq_sop/; Kozich et al., 2013). In short, sequences were binned into operational taxonomical units (OTUs) at a 97% sequence identity level using the OptiClust method (Westcott and Schloss, 2017) and classified against the SILVA (v.132) database (Quast et al., 2012), following quality and chimera checks (uchime v 4.2 http://www.drive5.com/uchime). Sequences related to chloroplasts, mitochondria, Eukaryota, or classified as 'unknown' (at the domain level) were also removed.

Downstream analyses (alpha/beta diversity) were performed on a local machine (macOS; mothur v1.48). Samples were sub-sampled down to 40 206 reads either before or during diversity analyses (see below), resulting in the

195 exclusion of 5 samples from the 2018 dataset; the final dataset therefore contained 31 samples from 2015, 3 from

196 2017 and 8 from 2018 (including replicates; Table 1). Both measures of alpha and beta (Bray-Curtis dissimilarity)

197 diversity were calculated with default settings; averages from sub-sampling iterations (1000) were used in both

198 cases. Distances in Bray-Curtis dissimilarities were visualised as ordinations using principal coordinate analyses

199 (PCoA) and non-metric multidimensional scaling (nMDS) calculated in mothur. Full details on the specific

200 mothur commands used are provided as Supplementary Information.

2.6 LEfSe analyses

202 One aim of the present study was to assess potential changes in microbial assemblages exported in proglacial

203 runoff over different stages of melt during the ablation season as the hydrological drainage system of LG

204 undergoes re-configuration (e.g. distributed to efficient). To identify which major OTUs (LDA scores > 3.5, p-

205 value < 0.01) were over- or under- represented during six different hydrological periods at LG (see Results section

206 below), we used linear discriminant analysis effect size (LefSe) implemented in mothur (v.1.44.3). Relative

207 changes in relative abundance across all samples for the identified OTUs were then visualised as a heatmap.

2.7 Identification of methane-cycling populations

209 A detailed characterisation of methane-cycling communities at LG is beyond the scope of the present study.

210 However, major clades of both methanotrophic and methanogenic populations from subglacial outflows in the

211 same GrIS sector have been described previously (Vrbická et al., 2022; Lamarche-Gagnon et al., 2019; Dieser et

212 al., 2014; Stibal et al., 2012; Znamínko et al., 2023). Based on these previous reports, we herein define putative

213 methanotroph bacterial populations as OTUs of the genera *Methylobacter* and *Crenothrix* (Znamínko et al., 2023),

214 and putative methanogen populations as OTUs of the orders Methanobacteriales, Methanomicrobiales,

215 Methanosarcinales (Lamarche-Gagnon et al., 2019). Screening for methanogenic populations also revealed a

216 relatively high abundance of reads classified as the anaerobic methane-oxidising archaea *Candidatus*

217 *methanoperedens* (Cai et al., 2018) amongst the Methanosarcinales in some samples. OTUs classified as *C.*

218 *methanoperedens* were therefore also included as potential methane-oxidising archaea.

2.8 Data manipulation and visualisation

220 Unless stated otherwise, all data manipulation and visualisation were performed in R (v. 4.2.1, R Core Team,

221 2013) utilised through RStudio (v. 2023.06.2, R Studio Team, 2020) using packages from the Tidyverse

222 (Wickham et al., 2019).

223

224 **Table 1: Summary of number of water (Sterivex) and bioinformatics samples**

Melt season	Time Span	Sterivex Samples	Bioinfo. Samples	Bioinfo. Replicate	Time Points*	Hydrological Period	Primer Pair**	Dataset
2015	4 – 13 May	4	3	1	3	borehole	Caporaso 2011	Lamarche-Gagnon et al. 2019
2015	7 June 2015	2	2	2	1	early-melt	Caporaso 2011	Lamarche-Gagnon et al. 2019
2015	20 June – 10 July	30	20	2-3	7	outburst	Caporaso 2011	Lamarche-Gagnon et al. 2019
2015	13-26 July	11	6	1-3	3	peak-flow	Caporaso 2011	Lamarche-Gagnon et al. 2019
2017	5 Sept	3	3	3	1	late-melt	Caporaso 2011	Kohler et al. 2020
2018	24 June – 24 July	8	8	1-2	7	transition	Parada-Apprill 2016-15	Vrbická et al. 2022

225 Sterivex samples correspond to the number of Sterivex filters collected and subjected to DNA extraction. Bioinformatics samples
226 correspond to the number of DNA samples sequenced. Bioinformatics replicates correspond to the number of replicate samples
227 for each group of samples. See Table S2 for details.
228 *In 2015, samples were collected on 17 separate days, but three sets of samples were pooled into single samples prior to
229 sequencing resulting in 14 sets of samples. The 2018 dataset here contains one sample per day except for 25 June 2018, which
230 was sampled twice at ~3 hr intervals (see methods/Table S2).
231 ***The V4 (515-806) primer pair used during Illumina MiSeq sequencing. Caporaso 2011 refers to the Caporaso et al. (2011)
232 primer pair and the Parada-Apprill 2016-15 refers to the Parada et al. (2016) 515F-Y and Apprill et al. (2015) 806R primer pair
233 (see methods).
234

3 Results

3.1 The hydrological evolution of the LG proglacial river (water sourcing)

The hydrology and hydrochemistry of the LG river reflect the status of its drainage system and can therefore inform on the sourcing of proglacial waters and their suspended material. To interpret changes in sampled microbial assemblage structure within the context of their upstream sources beneath or over the ice, we re-visit previously described hydrological and hydrochemical data at LG (Kohler et al., 2017; Hatton et al., 2019; Hawkings et al., 2021b). Figure 1 puts microbiological sampling in the context of the hydrological status of LG based on our understanding of its drainage system. Based on changes in runoff hydrochemistry (e.g. Hatton *et al.* 2019), flow regime, and SSC, we separate microbiological samples into six different "hydrological periods" or categories between the three years of sampling:

1. <u>Boreholes:</u> In 2015, the first set of samples were collected prior to the melt onset and consisted of relatively stagnant water accessed via boreholes through naled river-ice (see methods) and hereafter referred to as "2015 borehole" samples (4-13 May 2015; n = 3). This set of samples were the only samples that did not consist of flowing waters (i.e. runoff), but most likely consisted of a mixture of over-wintered late-runoff from the previous year (i.e. storage waters) and basal meltwaters (e.g. Graly and Rezvanbehbahani, 2023). These waters contained relatively high methane concentrations ($\sim 4\ \mu M$), were hypoxic (25.8 μM or < 6% air saturation) and contained very little suspended sediment but overall higher dissolved ion concentrations than bulk runoff (Table S1; Hatton et al. (2019)).

2. <u>Early melt period:</u> The second set of 2015 samples consisted of runoff samples collected during the early melt season (7 June 2015; n = 2). At this point in the season, the glacial hydrological system was poorly developed, and most waters exiting the glacier consisted of over winter stored basal meltwaters from/near the margin of the glacier (Bartholomew et al., 2011; Kellerman et al., 2020). These waters were more diluted by surface and englacial melt than the borehole samples, but still showed low SSC and relatively high EC, solute and CH_4 concentrations compared to the rest of the of the runoff samples, indicative of less dilution by surface melt than later in the season (Lamarche-Gagnon et al., 2019; Hatton et al., 2019).

3. <u>Outburst period:</u> The highest number of microbial samples in 2015 spanned a period where the LG hydrological drainage systems was undergoing rapid spatial expansion following the "spring event" (e.g. Mair et al., 2003), between 19 June – 15 July 2015 ("2015 outburst" samples; n = 20). This period has been extensively described in previous studies (Hawkings et al., 2018; Lamarche-Gagnon et al., 2019; Hatton et al., 2019; Kohler et al., 2020; Kellerman et al., 2020). In short, the series of four pulses (outbursts) in Q and SSC (Fig. 1) during that period reflect the rapid drainage of supraglacial waters to the base of the glacier (Bartholomew et al., 2011). This large input of dilute surface meltwater mechanically disrupts the glacier's subglacial hydrology, flushing out waters with high sediment (and CH_4) loads from newly connected sectors of the glacier's bed (Bartholomew et al., 2011; Lamarche-Gagnon et al., 2019).

4. <u>Peak flow period</u>: The last set of of microbial samples in 2015 were collected directly following the outburst period (15 – 23 July) during peak flow ("2015 peak flow" samples; n = 6). The drainage system then experienced full spatial extent where surface meltwaters quickly transit through efficient subglacial drainage conduits before exiting the ice, reflected by the drop in SSC, relatively low EC, and high Q (Fig. 1; Hatton et al., 2019; Chandler et al., 2021; Chandler et al., 2013).

5. <u>Late-melt period</u>: The 2017 samples ("2017 late-melt") were collected towards the end of the melt season (Kohler et al., 2020). Whilst no continuous hydrological LG data is available for 2017, the Watson River hydrograph indicates that the LG samples were collected just prior to the shutdown of the LG hydrological system during a time of flow recession (Fig. 1). Runoff at this time is inferred to mostly flow through pre-existing channels developed earlier during the melt season (Davison et al., 2019).

6. <u>2018 transition period</u>: The 2018 set of samples were collected during the same time period as the "outburst period" in 2015 (24 June to 11 July 2018; Vrbická et al., 2022), a few weeks following the putative spring event (7 June) but before peak flow (22 July; Fig. 1). However, no clear indication of outburst hydrological pulses occurred during the sampling period (Hawkings et al., 2021b; Vrbická et al., 2022). While Q decreased over the first week in June before increasing steadily during the July period, SSC decreased over the entire sampling period (Fig. 1). Because no distinctive hydrological or hydrochemical events characterised the 2018 sampling period, we group all of the microbial samples collected in 2018 into a single hydrological period: "2018 transition period"; n = 8.

The number of microbiological samples from each dataset and hydrological period is summarised in Tables 1 and S2.
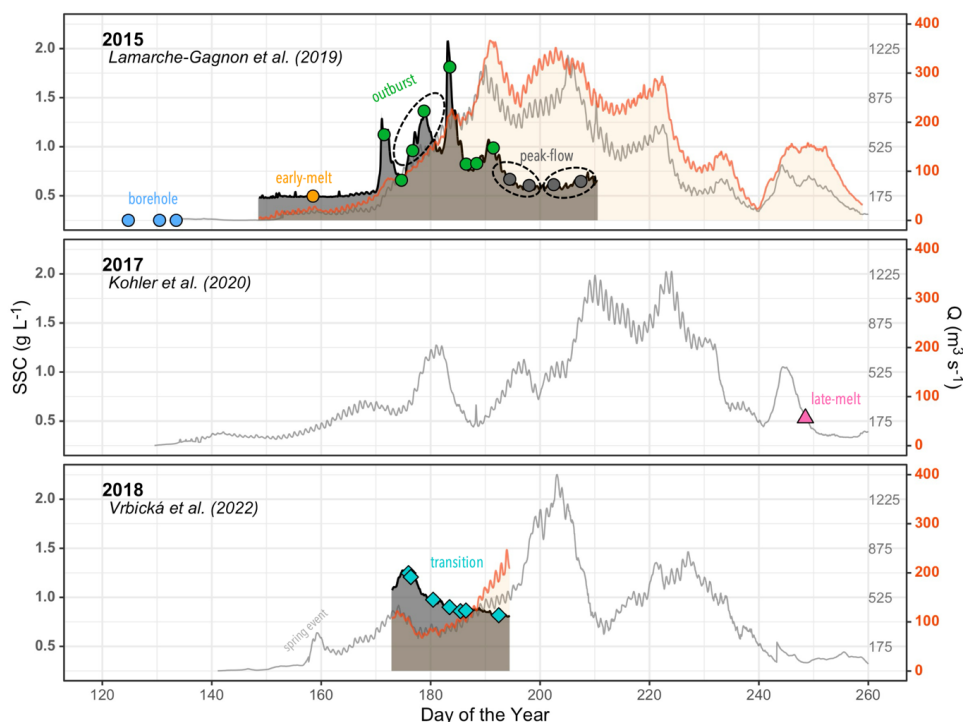
Figure 1: Hydrological and hydrogeochemial evolution of the LG proglacial river for the 3 years of sampling. Dark-grey and orange ribbon timeseries respectively correspond to suspended sediment concentration (SSC) and discharge (Q) at LG; no Q or SSC data in 2017 and limited data in 2018. Light grey line timeseries correspond to the Watson River discharge measured ~25 km downstream (data from Van As, 2022). Coloured points overlayed onto the SSC (2015, 2018) or Watson River Q (2017) timeseries indicate the sampling time of waters used for DNA extraction (Sterivex filters). Fill colours correspond to the six different hydrological periods identified (see Results). In 2015, dashed elipses highlight samples that have been merged from different sampling days prior to sequencing (see Table 1, S2). References for the original microbial datasets used are identified beneath the melt season year.

3.2 Microbial diversity and composition
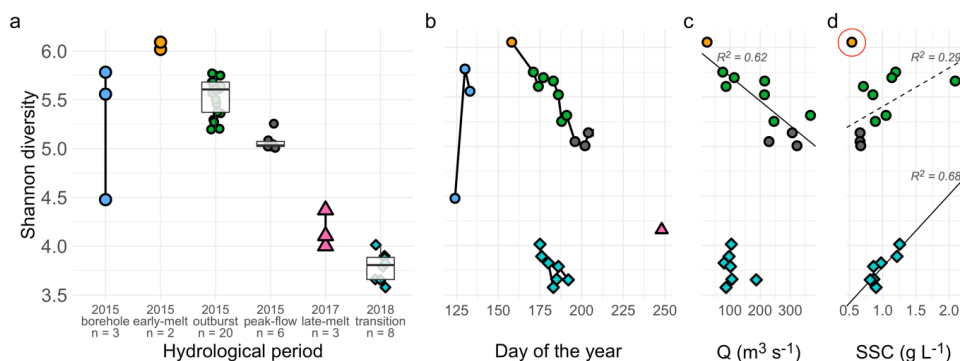
Figure 2: Shannon alpha diversity. (a) Shannon alpha diversity separated by hydrological period. All replicate samples are displayed; when n > 3, boxplots displays median, interquartile range (IQR; box) and 1.5 X IQR (whiskers). (b) Shannon diversity versus day of the year. Averages between replicates are shown with range displayed as vertical error bar (when larger

312 than point). Horizontal error bars are only barely visible for the last 2015 data point, and present for sample points derived
313 from multiple sampling days (see methods; Table S2). Points of the same dataset are linked by black line; for the 2015 dataset,
314 borehole (blue) and runoff samples (rest) are separated. (c) Shannon diversity versus discharge (Q) and (d) suspended sediment
315 concetration (SSC) for runoff samples; averages of replicates displayed. In c-d, solid black line display significant (p < 0.05)
316 correlations whereas the dashed line in (d) displays a weak, though non-significant, correlation in 2015 when exluding the
317 early-melt samples (orange point, circled in red). Same y-axis, fill colour and shape scheme is used in all panels.

318

319 In terms of microbial alpha-diversity (diversity within samples), samples from the 2015 dataset had the highest

320 number of reads (pre-subsampling), OTUs, and Shannon and inverse-Simpson diversity amongst all datasets

321 (Table S3, Fig. S2). The 2015 samples also showed a wider range of alpha-diversity than the 2018 transition and

322 2017 late-melt samples, in line with the wider range of hydrological periods (and overall higher number of

323 samples) captured during the 2015 melt season (Fig. 2, Fig. S2). Late-melt 2017 samples exhibited lower alpha-

324 diversity than the 2015 samples, but were higher than the 2018 samples. Diversity in runoff samples generally

325 decreased over the sampling period in both 2015 and 2018, even if it was more pronounced for the 2015 dataset

326 (Fig. 2; Vrbická et al., 2022). However, whereas this deceasing trend was correlated with increasing Q in 2015,

327 no such trend was present in 2018. Instead, Shannon diversity in 2018 was positively correlated with SSC; for the

328 2015 samples a weak, though not significant (p-value > 0.05), correlation with SSC was also observed, but only

329 when excluding the early-melt samples (Fig. 2 d).

330
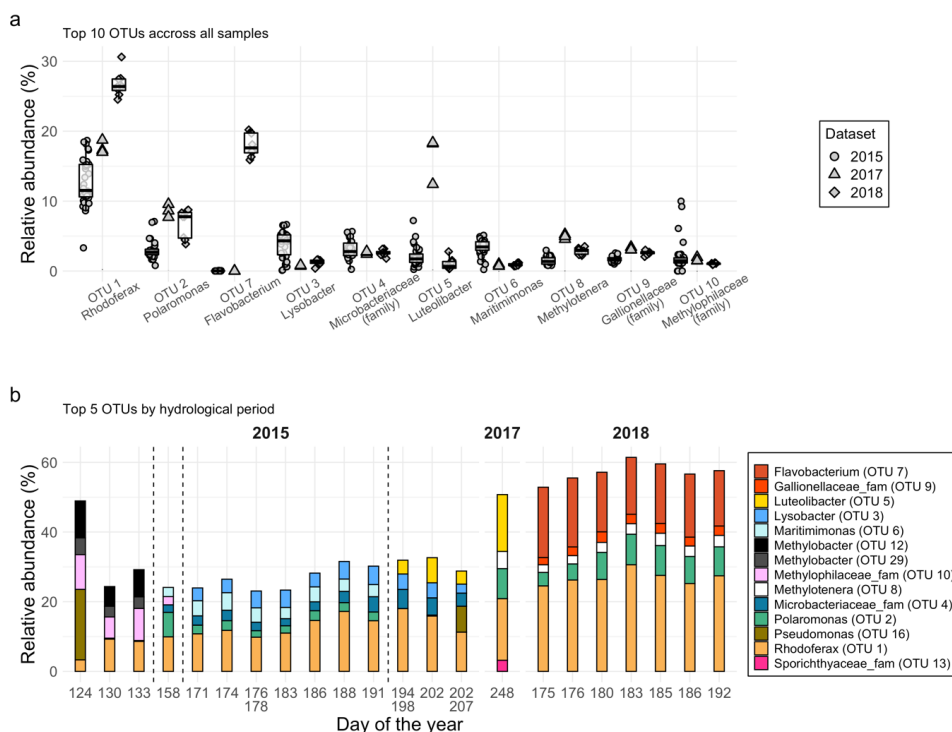
331

332 **Figure 3: Relative abundance of major OTUs.** (a) Relative abundance of the most abundant OTUs (top 10) across all
333 samples. Datasets are plotted separately with all replicate samples displayed. For 2015 and 2018 datasets, boxplots displays
334 median, interquartile range (IQR; box) and 1.5 X IQR (whiskers). On the x-axis, OTUs are ordered by relative abundance
335 across all samples, and OTU number and genus of the representative sequence displayed when possible; when the genus of

336 the OTU could not be classified, family is displayed instead. (b) Relative abundance of the most abundant (top 5) OTUs by
337 hydrological period. Average relative abundance of replicate samples are displayed. Vertical dashed lines in 2015 separate the
338 different hydrological periods. In 2015, a double day on the x-axis corresponds to samples that have been derived from two
339 separate days (see methods; Fig. 1, Table S2).
340

341 Looking at microbial assemblage composition, notable differences were also observed amongst the main OTUs

342 characterising the different hydrological periods. Whilst the most abundant (top ~2%) OTUs across all samples

343 were shared across all datasets (2015-18), there was a marked difference in their relative abundance between

344 datasets and hydrological periods. For example, the top 5 OTUs in 2017 and 2018 accounted for more than 50 %

345 of assemblage total relative abundance, while in 2015, they generally contributed up to ~30% (Fig. 3b). A marked

346 difference here were OTU 5 (*Luteolibacter*) and OTU 7 (*Flavobacterium*), which accounted for ~ 16-18 % of all

347 reads in 2017 and 2018 reads, respectively, but were nearly absent (< 0.01 % of dataset; OTU 7) or in much lower

348 relative abundance (1-2 % of dataset; OTU 5) in the 2015/17 and 2015/18 datasets, respectively (Fig. 3). OTUs

349 related to *Methylobacter* (OTUs 12 and 29) were also overrepresented in the borehole and last set of 2015

350 samples (Fig. 3b).

351

352 Trends in beta-diversity (diversity between samples) better highlighted temporal changes in exported microbial

353 community structure over the different sampling periods. Different groupings between samples, hydrological

354 periods, and datasets are apparent on the PCoA and nMDS projections of Bray-Curtis dissimilarity (Fig. 4a, b).

355 The most distinct communities were present in the 2015 borehole samples, but they were still more closely related

356 to 2015 runoff samples than those collected in late 2017 and 2018, with separations between datasets most notable

357 along the x-axis of ordination projections (Fig. 4a, b). Similar to alpha-diversity variations, the largest shifts in

358 communitiy structures were observed for the 2015 dataset, again likely reflecting the larger spread of hydrological

359 periods captured during the 2015 melt season (Fig. 1). A smaller, though relatively steady, temporal progression

360 was also observed for the 2018 samples (Fig. 4, b; Vrbická et al., 2022).
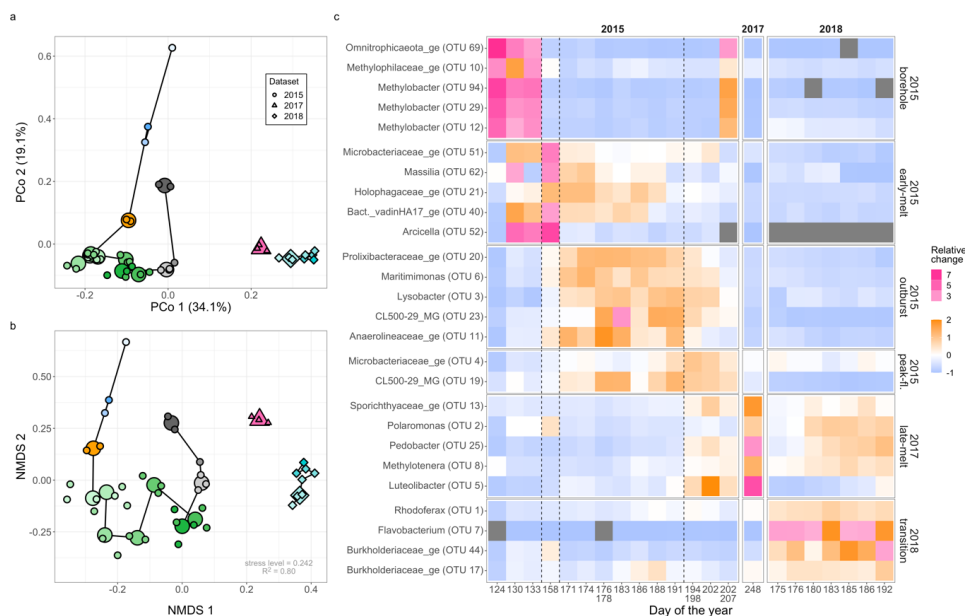
361

362 **Figure 4: Visualisation of microbial beta-diversity.** Ordinations of principle coordinates analysis (PCoA) (a) and non-metric
363 dimensional scaling (nMDS) (b) on Bray-Curtis distances, and relative change in relative abundance of major OTUs idenfitied
364 by Linear discriminant analysis effect size (LEfSe) (c). In a, b, shapes and colours correspond to the different hydrological
365 periods and datasets respectively, as per Fig. 1-2. Smaller points represent individual replicate samples and larger points
366 averages. Black lines link samples by sampling day for the 2015 and 2018 datasets (averaged points are linked when replicate
367 samples are present). The colour gradient represents earlier (lighter) and later (darker) sampling days for each hydrological
368 period. In (c), the heatmap displays relative changes in relative abundance accross the entire sample set. Two separate colour
369 schemes are used to highlight trends for the more subtle changes in relative abundance (relative changes larger or smaller than
370 2); white indicates no relative change relative to entire sample-set average for that OTU, blues decreases in relative abundance
371 relative to sample-set average and oranges and pinks increases in relative abundance relative to sample-set average. Dark grey
372 tiles indicate absence of OTU in the sample. Only up to 5 OTUs per hydrological period (LEfSe class) are displayed (highest
373 LDA score per LEfSe class; Table S4). Horizontal dashed lines separates hydrological periods on the x axis. Silva taxonomical
374 classification of OTU representative sequences down to the genus level (when possible) displayed on the y axis (Table S5 for
375 details).
376

377 We used LEfSe analysis to gain additional insight into the main microbial populations driving the differences in
378 assemblage structure during the different hydrological periods identified. Looking at the relative change in relative
379 abundance of these populations between all samples, we can see that specific OTUs were overrepresented during
380 the different hydrological periods sampled (Fig. 4.c). LEfSE analysis reinforced trends highlighted in some of the
381 most abundant OTUs identified above (Fig. 3), such as an overrepresentation of *Flavobacteria* (e.g. OTU 7) in
382 the 2018 samples, *Luteolibacter* (OTU 5) in late 2017 and methylotrophic and methanotrophic clades (e.g.
383 *Methylobacter*) in the 2015 borehole and the last set of 2015 samples (Fig. 4c). Additionnally LEfSe also
384 highlighted a relative increase in OTUs related to specific ecological niches during the different hydrological
385 periods sampled. For instance, a notable prevalence of OTUs related to (falcultative) anaerobes (e.g.
386 Anaerolineales, OTU 11) or to sequences from anoxic systems (e.g. OTUs 20, 23) during the 2015 outburst period,
387 versus OTUs related to taxa typically associated with more oxic environment (e.g. OTU 25), or those found on
388 glacier's surfaces (e.g. OTUs 4, 7), overrepresented in samples from the 2015 peak-flow, 2017 late-melt, and 2018
389 transition periods (Fig. 4c; Table S5).
390

391

4 Discussion

393 The differences in microbial assemblages observed at LG between the different hydrological periods likely reflect
394 contrasts in catchment water and sediment that principally supply the proglacial river at the time of sampling. The
395 exact state of the glacier's hydrological system (i.e. water/solute sourcing and flowpaths) is difficult to infer and
396 varies during and between seasons (e.g. when comparing 2015 and 2018 hydrological data during overlapping
397 time periods; Fig. 1). Broadly speaking, water origin will develop from a higher proportion of basal and
398 subglacially-stored melt earlier in the season, to a predominant contribution of (subglacially routed) surface
399 meltwaters as the melt season progresses (e.g. Bartholomew et al., 2011; Chandler et al., 2013; Kellerman et al.,
400 2020; Hatton et al., 2019). These variations in water sourcing and routing can explain the observed differences
401 in microbial assemblage structure; these are discussed in more details below.
402

403 Early-season meltwaters more likely comprise a mix of groundwater, basal meltwater and stored surface melt
404 from the previous season retained beneath the ice following drainage system shut down, that would have
405 undergone biogeochemical transformation overwinter (Kellerman et al., 2020; Dubnick et al., 2023). These are

406 inferred to be stored in disconnected cavities, or water-saturated subglacial sediments closer to the ice margin

407 over-winter, and mobilised by new supply of meltwater from the ice sheet surface in spring (Chu, 2014).

408

409 More vigourous and episodic flushing of subglacial environments during outburst events mobilises more spatially

410 disparate sectors of the bed, but additionally likely mixes thicker layers of subglacial sediments encompassing a

411 broader range of environmental conditions (e.g. (micro)oxic-anoxic transition zones; Hodson et al. (2008)). In

412 2015, these outburst events were also accompanied by CH_4 pulses, indicating the flushing of methane-rich sectors

413 of the glacier's bed (i.e likely anoxic; Lamarche-Gagnon et al. (2019)). These geochemical patterns are consistent

414 with the increase in the relative abundance of putative anaerobic taxa exported to the ice margin during that period

415 (Fig. 4c; Table S4-S5), including methanogens (Fig. S3; see section below). As the glacier area experiencing

416 surface melting expands with snowline retreat, surface meltwaters enter the subglacial environment via moulins

417 at locations increasingly distant from the ice margin, and the evacuation of subglacial material from more remote

418 subglacial sources is indicated by the export of older particulate organic carbon (POC) within suspended

419 sediments during this period (Kohler et al., 2017). In short, the mobilisation of subglacial material from more

420 heterogeneous sources earlier in the melt season and during outburst events likely explains the overall higher

421 microbial diversity observed during those periods (Fig. 2a).

422

423 Similarly, a shift towards more streamlined and efficient flowpaths draining the glacier later in the melt season

424 likely explains the overall decrease in alpha-diversity with increasing Q in 2015 but also the relatively lower

425 diversity during late-melt in 2017 (Fig. 2). Following the 2015 outburst period, meltwaters are mostly flowing

426 through an already well-developed, hydrologically efficient drainage system where surface meltwaters rapidly

427 transit from the ice surface, to hydrologically efficient subglacial flowpaths, to the ice margin, and finally to the

428 proglacial zone (Chandler et al., 2013; Hatton et al., 2019; Chandler et al., 2021). This rapidly transiting surface

429 meltwater dilutes the contribution of subglacial waters with more prolonged contact with the sediments at the ice

430 sheet bed (e.g. slow and inefficiently routed and stored meltwaters). Towards the end of the ablation season (e.g.

431 2017 samples), surface melt input decreases but meltwaters continue to flow through an efficient subglacial system

432 previously developed earlier that summer that have not yet collapsed from ice overburden pressure (Davison et

433 al., 2019). Therefore, once the subglacial environment has been extensively flushed and drainage system

434 established and stabilised, we can expect a higher proportion of exported microbial assemblages to be derived

435 from glacial surfaces, as well as to consist of more stable and widespread (sub)glacial populations (e.g. putative

436 generalists; Dubnick et al., 2023). This is reflected here by a relative increase during these periods in OTUs related

437 to bacterial populations commonly found on glacial surfaces and/or reported in (sub)glacial systems more broadly

438 (e.g. OTUs 1 (*Rhodoferax*), 2 (*Polaromonas*), 4 (*Microbacteriaceae*), 5 (*Luteolibacter*), 25 (*Pedobacter*); Fig. 4,

439 Table S5; e.g. Zhang et al. (2012), Andrews et al. (2018), Kohler et al. (2020), Doyle and Christner (2022), Rathore

440 et al. (2022), Bradley et al. (2023), Dubnick et al. (2023)).

441

442 A very similar trend in beta-diversity progression linked to relative increased surface-related microbial

443 populations following melt-season progression has been reported in a another, smaller, GrIS catchment in South

444 Greenland (Dubnick et al., 2017). Sampling of a proglacial river on Disko Island (West Greenland) during late

445 August also revealed relatively high porportions of OTUs related to glacier surfaces in the microbial make-up of

446   the proglacial assemblages (Žárský et al., 2018). Overall, these results indicate that the composition of microbial

447   assemblages exported from the catchment is not only a function of discharge, but further highlights the importance

448   of timing, as microbial assemblages collected during low discharge early in the season differs from those collected

449   towards the end of the season during similar discharge (Fig. 1, 2, 4).

450   **4.1 Microbial data inform on the state of the LG hydrological system**

451   There was a stark difference in assemblage composition between the 2018 and 2015 samples which were collected

452   during the same time period. The most apparent microbal feature which sets the 2018 samples appart was the very

453   high relative abundance of populations from the order Flavobacteriales (respectively 21%, 4%, and 1% of all reads

454   from the 2018, 2015, and 2017 dataset; e.g. OTU7 Fig. 3). Nearest BLAST relatives of the most abundant

455   Flavobaceteriales OTU (OTU 7) are found in cryoconite hole sequences; i.e. glacial surface populations (Table

456   S5). Moreover, there was a lot of overlap in other OTUs overrepresented in the 2018 samples with those

457   highlited above for the 2015 peak-flow and 2017 late-melt samples (e.g. OTUs 1, 2, 4, 25); i.e. OTUs related to

458   glacial surfaces and/or widely reported glacial populations (Fig. 4, Table S5). The 2018 samples also exhibited

459   the lowest levels of alpha-diversity (Fig. 2). These microbial data suggest that at the time of sampling, a larger

460   component of microbial sequences were sourced from glacier surfaces and/or a smaller component from more

461   remote or heterogenously dispersed subglacial sediments in 2018 than at a similar time in 2015.

462

463   By taking a wider look at the overall 2018 melt season, it appears as if the 2018 sampling period occurred during

464   a slowdown or stasis in hydrological expansion for that sector of the ice sheet. The main melt onset (spring event)

465   in 2018 at LG seemed to have occurred around the 7 June 2018 (peak on the Watson hydrograph on day 158, Fig.

466   1), with discharge initially falling during the microbiological sampling period, and only increasing in intensity

467   toward the end of the sampling period (Fig. 1). This 2018 melt hiatus is likely explained by the relatively colder

468   air-temperatures in 2018 during the sampling period compared to previous seasons (Fig. S4). Of note is also the

469   lower pH recorded during the 2018 sampling period (pH ~ 6.5-7.5) compared to previous years at LG (pH ~ 7.2

470   – 9.8 over the same period; Fig. S5). Higher pH appears to be reflective of waters transiting through a subglacial

471   system where active physical erosion has produced an abundance of freshly comminuted reactive rock flour

472   conducive to rapid silicate hydrolysis and carbonation – this usually occurs during periods of increasing discharge

473   (Hatton et al., 2019). As such, the 2018 observation period is likely more analogous to a period following a

474   subglacial outburst or spring event, when surface waters flow subglacially through sectors of the bed with efficient

475   well-established subglacial drainage pathways that have been already flushed earlier in the melt season, although

476   closer to the ice-margin than during peak flow following the outbusrt period.

477

478   Similar to the 2018 dataset, Flavobacteriales also represented a large percentage of LG runoff microbial sequences

479   collected during the 2012 melt season (May-September 2012; Cameron et al. (2017)). Given that 2012

480   corresponded to a historic record melt year in Greenland (Nghiem et al., 2012), and that more than half of the

481   Cameron et al. (2017) microbial dataset was collected following the 2012 outburst period and the record 2012

482   surface melt pulse, the high abundance of Flavobacteriales sequences reported there for LG might also reflect the

483   relatively large input of ice surface microbial populations in the LG runoff dataset at that time. Note here that the

484   relatively high surface contribution in 2018 (and 2012) is a relative interpretation comparative to other melt

485   seasons at the same site, and that the microbial make-up sampled at LG still bears an overall "subglacial imprint",

486   especially when compared to other glacial rivers in the region (see Vrbická et al. (2022)).

487   **4.2 Trends in methane-cycling populations at LG**

488   Both methanogenic and methanotrophic populations identified here have been reported previously in the context

489   of methane export from the LG catchment (Lamarche-Gagnon et al., 2019). A closer look at the temporal trends

490   in their relative abundance sheds some light onto their distribution beneath the ice. The relative abundance of

491   methanotrophic populations was highest in borehole samples beneath the river ice in front of LG (~10-20% of

492   reads; Fig S3). This is consistent with the relatively high methane concentrations, reduced O_2 availability and

493   stable conditions *in situ* (Table S1). How widespread these conditions are beneath the ice sheet, however, is

494   unclear, but very similar methane-oxidizing populations have been reported for example in the (micro)oxic and

495   methane-rich water and sediment layers of subglacial lakes in Antarctica (Davis et al., 2023; Achberger et al.,

496   2016). Near identical methanotrophic populations were also overrepresented in small methane-rich subglacial

497   outflows of the same GrIS sector throughout the 2012, 2018 and 2019 melt seasons (Dieser et al., 2014; Znamínko

498   et al., 2023). Unlike for the LG river here, however, these relatively smaller outflows drain much smaller areas of

499   the bed constrained near the ice margin and might not be representative of ice sheet environments at large

500   (Hawkings et al., 2021b).

501

502   In 2015, the relative abundance of methanotrophs sharply decreased during the early-melt and outburst periods at

503   LG (Fig. S3, 4c), when subglacial waters from more remote sectors of the glacier bed were being progressively

504   accessed. An increase in relative abundance then occurred in the last set of 2015 samples (26 July) when waters

505   were rapidly transiting from the glacier's surface to the margin in well-established subglacial conduits (*see above*

506   *section*s). A very similar trend in relative abundance between aerobic methanotrophic bacteria and putative

507   anaerobic methane-oxidising archaea was observed in 2015 (Fig. S3), suggesting that if anaerobic methane

508   oxidisers are present beneath the ice, they might occupy a similar niche to aerobic methanotrophic populations,

509   perhaps relying on oxidised iron (which is likely in adundance; Hawkings et al. (2014)) as terminal electron

510   acceptor (Cai et al., 2018). Almost inversely, an increase in methanogen relative abundance was observed during

511   the 2015 othe early-melt and outburst periods, which aligns with the methane pulses observed during these periods

512   (Lamarche-Gagnon et al., 2019). In 2018, methanotrophic bacteria accounted for a larger proportion of

513   assemblages than in most of the 2015 runoff samples (Fig. S3). As discussed above, waters sampled in 2018 were

514   likely rapidly transiting in established efficient subglacial flowpaths, likely closer to the ice-margin than at a

515   similar period in 2015. Together, these temporal changes in relative abundance suggest that subglacial

516   methanotrophic niches may be constrained to the ice margin or (flanking) efficient drainage flowpaths in that

517   sector of the GrIS, with methanogenic hotspots in deeper sediments beneath the ice-rock interface.

518   **5 Conclusion**

519   The trends and differences in microbial composition during and between melt seasons observed here highlight

520   that the timing of sampling can influence the conclusions one can derive from spot sampling, or even continuous

521   sampling during a short period of a melt season without a more complete overview of seasonal hydrology and

522 hydrochemistry. We show that sampling the microbial assemblage from the same site thoughout a melt season

523 and in multiple years can yield different results, primarily because of changing hydrological regime. Therefore,

524 depending on the information details desired during microbial investigation of these dynamics systems, a good

525 understanding of glacial hydrology and hydrochemistry might be critical in informing microbial data. This is

526 likely especially true in larger glacial catchments that also undergo more dramatic hydrological re-configuration

527 over and between melt seasons.

528 6 Code availability

529 mothur .logfiles and .batch files will be uploaded to the Dataverse repository associated to this manuscript prior

530 to publication (https://dataverse.no/dataverse/uit).

531 7 Data availability

532 7.1 Molecular data

533 Raw reads for the 2015 dataset are available from the NCBI Sequence Read Archive

534 (https://www.ncbi.nlm.nih.gov/sra) under BioProject PRJNA495593. Quality checked datasets for 2017 and 2018

535 have been deposited in the MG-RAST database (https://www.mg-rast.org/) under the accession number

536 MGP92375 and MGP104407 respectively.

537 7.2 Hydrological and hydrochemical data

538 Hydrological sensor data for the LG river in 2015 and 2018 (Q, SSC, pH, as well as electrical conductivity), can

539 be found at: https://zenodo.org/doi/10.5281/zenodo.4634279 (Hawkings et al., 2021a). Hydrochemical data for

540 the 2015 melt season can be found here: https://doi.pangaea.de/10.1594/PANGAEA.896788 (Hatton et al., 2018).

541 The discharge record from the Watson river can be found here: https://doi.org/10.22008/FK2/XEHYCM (Van As,

542 2022) and the automatic weather station PROMICE data can be found here:

543 https://doi.org/10.22008/FK2/IW73UU (How et al., 2022).

544

545 Hydrochemical data from the 2015 borehole water samples, as well as manual pH measurements from the LG

546 river for the years 2009, 2010, 2012 will be uploaded to the Dataverse repository associated to this manuscript

547 prior to publication (https://dataverse.no/dataverse/uit).

548 8 Author contribution

549 GLG, MS, AMBA, JH and JLW conceived the project. GLG, MS, JLW, JH, PK, JK, TJK, LB, JH, AB and JT

550 collected the samples. GLG, MS, PK, JK, TJK and JH performed the lab work. GLG performed the analyses with

9 Competing interests

554 One of the (co-)authors is a member of the editorial board of TC.

10 Acknowledgments

11 References

572 Achberger, A. M., Christner, B. C., Michaud, A. B., Priscu, J. C., Skidmore, M. L., Vick-Majors, T. J., , t. W. S.
573 T., Adkins, W., Anandakrishnan, S., Barbante, C., Barcheck, G., Beem, L., Behar, A., Beitch, M., Bolsey, R.,
574 Branecky, C., Carter, S., Christianson, K., Edwards, R., Fisher, A., Fricker, H., Foley, N., Guthrie, B., Hodson,
575 T., Jacobel, R., Kelley, S., Mankoff, K., McBryan, E., Mikucki, J., Mitchell, A., Powell, R., Purcell, A., Sampson,
576 D., Scherer, R., Sherve, J., Siegfried, M., and Tulaczyk, S.: Microbial Community Structure of Subglacial Lake
577 Whillans, West Antarctica, Frontiers in Microbiology, 7, 10.3389/fmicb.2016.01457, 2016.

578 Andrews, M. G., Jacobson, A. D., Osburn, M. R., and Flynn, T. M.: Dissolved Carbon Dynamics in Meltwaters
579 From the Russell Glacier, Greenland Ice Sheet, Journal of Geophysical Research: Biogeosciences, 123, 2922-
580 2940, 10.1029/2018JG004458, 2018.

581 Apprill, A., McNally, S., Parsons, R., and Weber, L.: Minor revision to V4 region SSU rRNA 806R gene primer
582 greatly increases detection of SAR11 bacterioplankton, Aquatic Microbial Ecology, 75, 129-137, 2015.

583 Bartholomew, I., Nienow, P., Sole, A., Mair, D., Cowton, T., Palmer, S., and Wadham, J.: Supraglacial forcing
584 of subglacial drainage in the ablation zone of the Greenland ice sheet, Geophysical Research Letters, 38, n/a-n/a,
585 10.1029/2011GL047063, 2011.

586   Beaton, A. D., Wadham, J. L., Hawkings, J., Bagshaw, E. A., Lamarche-Gagnon, G., Mowlem, M. C., and Tranter,
587   M.: High-Resolution in Situ Measurement of Nitrate in Runoff from the Greenland Ice Sheet, Environmental
588   Science & Technology, 51, 12518-12527, 10.1021/acs.est.7b03121, 2017.

589   Bradley, J. A., Trivedi, C. B., Winkel, M., Mourot, R., Lutz, S., Larose, C., Keuschnig, C., Doting, E., Halbach,
590   L., Zervas, A., Anesio, A. M., and Benning, L. G.: Active and dormant microorganisms on glacier surfaces,
591   Geobiology, 21, 244-261, https://doi.org/10.1111/gbi.12535, 2023.

592   Burns, R., Wynn, P. M., Barker, P., McNamara, N., Oakley, S., Ostle, N., Stott, A. W., Tuffen, H., Zhou, Z.,
593   Tweed, F. S., Chesler, A., and Stuart, M.: Direct isotopic evidence of biogenic methane production and efflux
594   from beneath a temperate glacier, Scientific Reports, 8, 17118, 10.1038/s41598-018-35253-2, 2018.

595   Cai, C., Leu, A. O., Xie, G.-J., Guo, J., Feng, Y., Zhao, J.-X., Tyson, G. W., Yuan, Z., and Hu, S.: A
596   methanotrophic archaeon couples anaerobic oxidation of methane to Fe(III) reduction, The ISME Journal, 12,
597   1929-1939, 10.1038/s41396-018-0109-x, 2018.

598   Cameron, K. A., Stibal, M., Hawkings, J. R., Mikkelsen, A. B., Telling, J., Kohler, T. J., Gözdereliler, E., Zarsky,
599   J. D., Wadham, J. L., and Jacobsen, C. S.: Meltwater export of prokaryotic cells from the Greenland ice sheet,
600   Environmental Microbiology, 19, 524-534, 10.1111/1462-2920.13483, 2017.

601   Caporaso, J. G., Lauber, C. L., Walters, W. A., Berg-Lyons, D., Lozupone, C. A., Turnbaugh, P. J., Fierer, N.,
602   and Knight, R.: Global patterns of 16S rRNA diversity at a depth of millions of sequences per sample, Proceedings
603   of the National Academy of Sciences, 108, 4516-4522, 10.1073/pnas.1000080107, 2011.

604   Chandler, D. M., Wadham, J. L., Nienow, P. W., Doyle, S. H., Tedstone, A. J., Telling, J., Hawkings, J., Alcock,
605   J. D., Linhoff, B., and Hubbard, A.: Rapid development and persistence of efficient subglacial drainage under 900
606   m-thick   ice   in   Greenland,   Earth   and   Planetary   Science   Letters,   566,   116982,
607   https://doi.org/10.1016/j.epsl.2021.116982, 2021.

608   Chandler, D. M., Wadham, J. L., Lis, G. P., Cowton, T., Sole, A., Bartholomew, I., Telling, J., Nienow, P.,
609   Bagshaw, E. B., Mair, D., Vinen, S., and Hubbard, A.: Evolution of the subglacial drainage system beneath the
610   Greenland Ice Sheet revealed by tracers, Nature Geoscience, 6, 195-198, 10.1038/ngeo1737, 2013.

611   Christiansen, J. R. and Jørgensen, C. J.: First observation of direct methane emission to the atmosphere from the
612   subglacial domain of the Greenland Ice Sheet, Scientific Reports, 8, 16623, 10.1038/s41598-018-35054-7, 2018.

613   Christner, B. C., Priscu, J. C., Achberger, A. M., Barbante, C., Carter, S. P., Christianson, K., Michaud, A. B.,
614   Mikucki, J. A., Mitchell, A. C., Skidmore, M. L., Vick-Majors, T. J., and the, W. S. T.: A microbial ecosystem
615   beneath the West Antarctic ice sheet, Nature, 512, 310-313, 10.1038/nature13667, 2014.

616   Chu, V. W.: Greenland ice sheet hydrology: A review, Progress in Physical Geography, 38, 19-54, 2014.

617   Clason, C. C., Mair, D. W. F., Nienow, P. W., Bartholomew, I. D., Sole, A., Palmer, S., and Schwanghart, W.:
618   Modelling the transfer of supraglacial meltwater to the bed of Leverett Glacier, Southwest Greenland, The
619   Cryosphere, 9, 123-138, 10.5194/tc-9-123-2015, 2015.

620   Cowton, T., Nienow, P., Bartholomew, I., Sole, A., and Mair, D.: Rapid erosion beneath the Greenland ice sheet,
621   Geology, 40, 343-346, 2012.

622   Davis, C. L., Venturelli, R. A., Michaud, A. B., Hawkings, J. R., Achberger, A. M., Vick-Majors, T. J.,
623   Rosenheim, B. E., Dore, J. E., Steigmeyer, A., Skidmore, M. L., Barker, J. D., Benning, L. G., Siegfried, M. R.,
624   Priscu, J. C., Christner, B. C., Barbante, C., Bowling, M., Burnett, J., Campbell, T., Collins, B., Dean, C., Duling,
625   D., Fricker, H. A., Gagnon, A., Gardner, C., Gibson, D., Gustafson, C., Harwood, D., Kalin, J., Kasic, K., Kim,

626   O.-S., Krula, E., Leventer, A., Li, W., Lyons, W. B., McGill, P., McManis, J., McPike, D., Mironov, A., Patterson,
627   M., Roberts, G., Rot, J., Trainor, C., Tranter, M., Winans, J., Zook, B., and the, S. S. T.: Biogeochemical and
628   historical drivers of microbial community composition and structure in sediments from Mercer Subglacial Lake,
629   West Antarctica, ISME Communications, 3, 8, 10.1038/s43705-023-00216-w, 2023.

630   Davison, B. J., Sole, A. J., Livingstone, S. J., Cowton, T. R., and Nienow, P. W.: The Influence of Hydrology on
631   the Dynamics of Land-Terminating Sectors of the Greenland Ice Sheet, Frontiers in Earth Science, 7,
632   10.3389/feart.2019.00010, 2019.

633   Dawes, P. R.: The bedrock geology under the Inland Ice: the next major challenge for Greenland mapping,
634   Geological Survey of Denmark and Greenland Bulletin, 17, 57-60, 2009.

635   Dieser, M., Broemsen, E. L., Cameron, K. A., King, G. M., Achberger, A., Choquette, K., Hagedorn, B., Sletten,
636   R., Junge, K., and Christner, B. C.: Molecular and biogeochemical evidence for methane cycling beneath the
637   western margin of the Greenland Ice Sheet, ISME J, 8, 2305-2316, 10.1038/ismej.2014.59, 2014.

638   Doyle, S. M. and Christner, B. C.: Variation in bacterial composition, diversity, and activity across different
639   subglacial basal ice types, The Cryosphere, 16, 4033-4051, 10.5194/tc-16-4033-2022, 2022.

640   Dubnick, A., Kazemi, S., Sharp, M., Wadham, J., Hawkings, J., Beaton, A., and Lanoil, B.: Hydrological controls
641   on glacially exported microbial assemblages, Journal of Geophysical Research: Biogeosciences, 122, 1049-1061,
642   10.1002/2016JG003685, 2017.

643   Dubnick, A. J., Spietz, R. L., Danielson, B. D., Skidmore, M. L., Boyd, E. S., Burgess, D., Dhoonmoon, C., and
644   Sharp, M.: Biogeochemical evolution of ponded meltwater in a High Arctic subglacial tunnel, The Cryosphere,
645   17, 2993-3012, 10.5194/tc-17-2993-2023, 2023.

646   Graly, J. A. and Rezvanbehbahani, S.: Geological and glacial-hydrologic controls on chemical weathering in the
647   subglacial environment, Annals of Glaciology, 1-6, 10.1017/aog.2023.56, 2023.

648   Graly, J. A., Drever, J. I., and Humphrey, N. F.: Calculating the balance between atmospheric CO_2 drawdown
649   and organic carbon oxidation in subglacial hydrochemical systems, Global Biogeochemical Cycles, 31, 709-727,
650   10.1002/2016gb005425, 2017.

651   Hatton, J. E., Hendry, K. R., Hawkings, J., Wadham, J., Kohler, T., Stibel, M., Beaton, A., Bagshaw, E., and
652   Telling, J.: Major ion and silicon isotope composition of glacial meltwaters, Leverett and Kiattuut glacier,
653   Greenland, PANGAEA [dataset], 10.1594/PANGAEA.896788, 2018.

654   Hatton, J. E., Hendry, K. R., Hawkings, J. R., Wadham, J. L., Kohler, T. J., Stibal, M., Beaton, A. D., Bagshaw,
655   E. A., and Telling, J.: Investigation of subglacial weathering under the Greenland Ice Sheet using silicon isotopes,
656   Geochimica et Cosmochimica Acta, https://doi.org/10.1016/j.gca.2018.12.033, 2019.

657   Hawkings, J., Linhoff, B., Wadham, J., Stibal, M., Lamborg, C., Carling, G., Lamarche-Gagnon, G., Kohler, T.,
658   Ward, R., Hendry, K., Falteisek, L., Kellerman, A., Cameron, K., Hatton, J., Tingey, S., Holt, A., Vinšová, P.,
659   Hofer, S., Bulínová, M., Větrovský, T., Meire, L., and Spencer, R.: Datasets for "Large subglacial source of
660   mercury from the southwestern margin of the Greenland Ice Sheet", Zenodo [dataset], 10.5281/zenodo.4634279,
661   2021a.

662   Hawkings, J. R., Wadham, J. L., Tranter, M., Raiswell, R., Benning, L. G., Statham, P. J., Tedstone, A., Nienow,
663   P., Lee, K., and Telling, J.: Ice sheets as a significant source of highly reactive nanoparticulate iron to the oceans,
664   Nat Commun, 5, 3929, 10.1038/ncomms4929, 2014.

665 Hawkings, J. R., Hatton, J. E., Hendry, K. R., de Souza, G. F., Wadham, J. L., Ivanovic, R., Kohler, T. J., Stibal,
666 M., Beaton, A., Lamarche-Gagnon, G., Tedstone, A., Hain, M. P., Bagshaw, E., Pike, J., and Tranter, M.: The
667 silicon cycle impacted by past ice sheets, Nature Communications, 9, 3210, 10.1038/s41467-018-05689-1, 2018.

668 Hawkings, J. R., Linhoff, B. S., Wadham, J. L., Stibal, M., Lamborg, C. H., Carling, G. T., Lamarche-Gagnon,
669 G., Kohler, T. J., Ward, R., Hendry, K. R., Falteisek, L., Kellerman, A. M., Cameron, K. A., Hatton, J. E., Tingey,
670 S., Holt, A. D., Vinšová, P., Hofer, S., Bulínová, M., Větrovský, T., Meire, L., and Spencer, R. G. M.: Large
671 subglacial source of mercury from the southwestern margin of the Greenland Ice Sheet, Nature Geoscience,
672 10.1038/s41561-021-00753-w, 2021b.

673 Henson, M. W., Lanclos, V. C., Faircloth, B. C., and Thrash, J. C.: Cultivation and genomics of the first freshwater
674 SAR11 (LD12) isolate, The ISME Journal, 12, 1846-1860, 10.1038/s41396-018-0092-2, 2018.

675 Hodson, A., Anesio, A. M., Tranter, M., Fountain, A., Osborn, M., Priscu, J., Laybourn-Parry, J., and Sattler, B.:
676 Glacial ecosystems, Ecological Monographs, 78, 41-67, 10.1890/07-0187.1, 2008.

677 How, P., Abermann, J., Ahlstrøm, A. P., Andersen, S. B., Box, J. E., Citterio, M., Colgan, W. T., Fausto, R. S.,
678 Karlsson, N. B., Jakobsen, J., Langley, K., Larsen, S. H., Mankoff, K. D., Pedersen, A. Ø., Rutishauser, A., Shield,
679 C. L., Solgaard, A. M., van As, D., Vandecrux, B., and Wright, P. J.: PROMICE and GC-Net automated weather
680 station data in Greenland (V11), GEUS Dataverse [dataset], doi:10.22008/FK2/IW73UU, 2022.

681 Kellerman, A. M., Hawkings, J. R., Wadham, J. L., Kohler, T. J., Stibal, M., Grater, E., Marshall, M., Hatton, J.
682 E., Beaton, A., and Spencer, R. G. M.: Glacier Outflow Dissolved Organic Matter as a Window Into Seasonally
683 Changing Carbon Sources: Leverett Glacier, Greenland, Journal of Geophysical Research: Biogeosciences, 125,
684 e2019JG005161, 10.1029/2019jg005161, 2020.

685 Kohler, T. J., Žárský, J. D., Yde, J. C., Lamarche-Gagnon, G., Hawkings, J. R., Tedstone, A. J., Wadham, J. L.,
686 Box, J. E., Beaton, A. D., and Stibal, M.: Carbon dating reveals a seasonal progression in the source of particulate
687 organic carbon exported from the Greenland Ice Sheet, Geophysical Research Letters, 6209-6217,
688 10.1002/2017GL073219, 2017.

689 Kohler, T. J., Vinšová, P., Falteisek, L., Žárský, J. D., Yde, J. C., Hatton, J. E., Hawkings, J. R., Lamarche-
690 Gagnon, G., Hood, E., Cameron, K. A., and Stibal, M.: Patterns in Microbial Assemblages Exported From the
691 Meltwater of Arctic and Sub-Arctic Glaciers, Frontiers in Microbiology, 11, 10.3389/fmicb.2020.00669, 2020.

692 Kozich, J. J., Westcott, S. L., Baxter, N. T., Highlander, S. K., and Schloss, P. D.: Development of a Dual-Index
693 Sequencing Strategy and Curation Pipeline for Analyzing Amplicon Sequence Data on the MiSeq Illumina
694 Sequencing Platform, Applied and Environmental Microbiology, 79, 5112-5120, 2013.

695 Lamarche-Gagnon, G., Wadham, J. L., Sherwood Lollar, B., Arndt, S., Fietzek, P., Beaton, A. D., Tedstone, A.
696 J., Telling, J., Bagshaw, E. A., Hawkings, J. R., Kohler, T. J., Zarsky, J. D., Mowlem, M. C., Anesio, A. M., and
697 Stibal, M.: Greenland melt drives continuous export of methane from the ice-sheet bed, Nature, 565, 73-77,
698 10.1038/s41586-018-0800-0, 2019.

699 Mair, D., Willis, I., Fischer, U. H., Hubbard, B., Nienow, P., and Hubbard, A.: Hydrological controls on patterns
700 of surface, internal and basal motion during three "spring events": Haut Glacier d'Arolla, Switzerland, Journal of
701 Glaciology, 49, 555-567, 10.3189/172756503781830467, 2003.

702 Nghiem, S. V., Hall, D. K., Mote, T. L., Tedesco, M., Albert, M. R., Keegan, K., Shuman, C. A., DiGirolamo, N.
703 E., and Neumann, G.: The extreme melt across the Greenland ice sheet in 2012, Geophysical Research Letters,
704 39, https://doi.org/10.1029/2012GL053611, 2012.

705   Pain, A. J., Martin, J. B., and Young, C. R.: Sources and sinks of CO2 and CH4 in siliciclastic subterranean
706   estuaries, Limnology and Oceanography, 64, 1500-1514, 10.1002/lno.11131, 2019.

707   Palmer, S., Shepherd, A., Nienow, P., and Joughin, I.: Seasonal speedup of the Greenland Ice Sheet linked to
708   routing of surface water, Earth and Planetary Science Letters, 302, 423-428,
709   https://doi.org/10.1016/j.epsl.2010.12.037, 2011.

710   Parada, A. E., Needham, D. M., and Fuhrman, J. A.: Every base matters: assessing small subunit rRNA primers
711   for marine microbiomes with mock communities, time series and global field samples, Environmental
712   Microbiology, 18, 1403-1414, 10.1111/1462-2920.13023, 2016.

713   Quast, C., Pruesse, E., Gerken, J., Peplies, J., Yarza, P., Yilmaz, P., Schweer, T., and Glöckner, F. O.: The SILVA
714   ribosomal RNA gene database project: improved data processing and web-based tools, Nucleic Acids Research,
715   41, D590-D596, 10.1093/nar/gks1219, 2012.

716   R Core Team: R: A Language and Environment for Statistical Computing, R Foundation for Statistical Computing
717   [code], 2013.

718   R Studio Team: RStudio: Integrated Development Environment for R, RStudio, PBC. [code], 2020.

719   Rathore, M., Sinha, R. K., Venkatachalam, S., and Krishnan, K. P.: Microbial diversity and associated metabolic
720   potential in the supraglacial habitat of a fast-retreating glacier: a case study of Patsio glacier, North-western
721   Himalaya, Environmental Microbiology Reports, 14, 443-452, https://doi.org/10.1111/1758-2229.13017, 2022.

722   Röthlisberger, H.: Water Pressure in Intra- and Subglacial Channels, Journal of Glaciology, 11, 177-203,
723   10.3189/S0022143000022188, 1972.

724   Schloss, P. D., Westcott, S. L., Ryabin, T., Hall, J. R., Hartmann, M., Hollister, E. B., Lesniewski, R. A., Oakley,
725   B. B., Parks, D. H., Robinson, C. J., Sahl, J. W., Stres, B., Thallinger, G. G., Van Horn, D. J., and Weber, C. F.:
726   Introducing mothur: Open-Source, Platform-Independent, Community-Supported Software for Describing and
727   Comparing Microbial Communities, Applied and Environmental Microbiology, 75, 7537-7541, 2009.

728   Stibal, M., Wadham, J. L., Lis, G. P., Telling, J., Pancost, R. D., Dubnick, A., Sharp, M. J., Lawson, E. C., Butler,
729   C. E. H., Hasan, F., Tranter, M., and Anesio, A. M.: Methanogenic potential of Arctic and Antarctic subglacial
730   environments with contrasting organic carbon sources, Global Change Biology, 18, 3332-3345, 10.1111/j.1365-
731   2486.2012.02763.x, 2012.

732   van As, D.: Watson River discharge (V1), GEUS Dataverse [dataset], doi:10.22008/FK2/XEHYCM, 2022.

733   Vrbická, K., Kohler, T. J., Falteisek, L., Hawkings, J. R., Vinšová, P., Bulínová, M., Lamarche-Gagnon, G., Hofer,
734   S., Kellerman, A. M., Holt, A. D., Cameron, K. A., Schön, M., Wadham, J. L., and Stibal, M.: Catchment
735   characteristics and seasonality control the composition of microbial assemblages exported from three outlet
736   glaciers of the Greenland Ice Sheet, Frontiers in Microbiology, 13, 10.3389/fmicb.2022.1035197, 2022.

737   Wadham, J. L., Hawkings, J. R., Tarasov, L., Gregoire, L. J., Spencer, R. G. M., Gutjahr, M., Ridgwell, A., and
738   Kohfeld, K. E.: Ice sheets matter for the global carbon cycle, Nature Communications, 10, 3567, 10.1038/s41467-
739   019-11394-4, 2019.

740   Wadham, J. L., Tranter, M., Skidmore, M., Hodson, A. J., Priscu, J., Lyons, W. B., Sharp, M., Wynn, P., and
741   Jackson, M.: Biogeochemical weathering under ice: Size matters, Global Biogeochemical Cycles, 24, n/a-n/a,
742   10.1029/2009gb003688, 2010.

743   Weertman, J.: General theory of water flow at the base of a glacier or ice sheet, Reviews of Geophysics, 10, 287-
744   333, https://doi.org/10.1029/RG010i001p00287, 1972.

745   Westcott, S. L. and Schloss, P. D.: OptiClust, an Improved Method for Assigning Amplicon-Based Sequence Data
746   to   Operational   Taxonomic   Units,   mSphere,   2,   10.1128/mspheredirect.00073-00017,
747   doi:10.1128/mspheredirect.00073-17, 2017.

748   Wickham, H., Averick, M., Bryan, J., Chang, W., McGowan, L. D. A., François, R., Grolemund, G., Hayes, A.,
749   Henry, L., Hester, J., Kuhn, M., Pedersen, T. L., Miller, E., Bache, S. M., Müller, K., Ooms, J., Robinson, D.,
750   Seidel, D. P., Spinu, V., Takahashi, K., Vaughan, D., Wilke, C., Woo, K., and Yutani, H.: Welcome to the
751   Tidyverse, Journal of Open Source Software, 4, 1686, 10.21105/joss.01686, 2019.

752   Žárský, J. D., Kohler, T. J., Yde, J. C., Falteisek, L., Lamarche-Gagnon, G., Hawkings, J. R., Hatton, J. E., and
753   Stibal, M.: Prokaryotic assemblages in suspended and subglacial sediments within a glacierized catchment on
754   Qeqertarsuaq (Disko Island), west Greenland, FEMS Microbiology Ecology, 94, fiy100-fiy100,
755   10.1093/femsec/fiy100, 2018.

756   Zhang, W., Zhang, G., Liu, G., Li, Z., Chen, T., and An, L.: Diversity of Bacterial Communities in the Snowcover
757   at Tianshan Number 1 Glacier and its Relation to Climate and Environment, Geomicrobiology Journal, 29, 459-
758   469, 10.1080/01490451.2011.581329, 2012.

759   Znamínko, M., Falteisek, L., Vrbická, K., Klímová, P., Christiansen, J. R., Jørgensen, C. J., and Stibal, M.:
760   Methylotrophic Communities Associated with a Greenland Ice Sheet Methane Release Hotspot, Microbial
761   Ecology, 10.1007/s00248-023-02302-x, 2023.
762